

Crystal Engineering of NLO Materials Based on Metal–Organic Coordination Networks

OWEN R. EVANS AND WENBIN LIN*

Department of Chemistry, CB#3290, University of North Carolina, Chapel Hill, North Carolina 27599

Received September 17, 2001

ABSTRACT

Crystal engineering, the ability to predict and control the packing of molecular building units in the solid state, has attracted much attention over the past three decades owing to its potential exploitation for the synthesis of technologically important materials. We present here the development of crystal-engineering strategies toward the synthesis of noncentrosymmetric infinite coordination networks for use as second-order nonlinear optical (NLO) materials. Work performed mainly in our laboratory has demonstrated that noncentrosymmetric solids based on infinite networks can be rationally synthesized by combining unsymmetrical bridging ligands and metal centers with well-defined coordination geometries. Specifically, coordination networks based on 3D diamondoid and 2D grid structures can be successfully engineered with a high degree of probability and predictability to crystallize in noncentrosymmetric space groups. We have also included noncentrosymmetric solids based on 1D chains and related helical structures for comparison.

Introduction

The field of crystal engineering is primarily concerned with the ability to predictably synthesize supramolecular structures from well-designed building blocks.¹ The organic solid-state community has strived to achieve the dream of rationally constructing functional supramolecular assemblies since Schmidt coined the term “crystal engineering” three decades ago.² To date, precise prediction of the structure of a molecular solid still is a daunting task, even with the most powerful computational approaches, because crystal packing is governed by many weak non-covalent intermolecular forces.³ The inability to predict the structure of even the simplest crystalline solids from a knowledge of their chemical composition has greatly hampered the progress of crystal engineering of functional solids.

Owen R. Evans was born in Kirkham, England, in 1975. He received his B. S. degree from Merrimack College, North Andover, Massachusetts. He is currently pursuing postdoctoral research with Professors T. D. Tilley and A. Bell at the University of California at Berkeley after receiving a Ph.D. degree in chemistry from Brandeis University, Waltham, Massachusetts in December 2001.

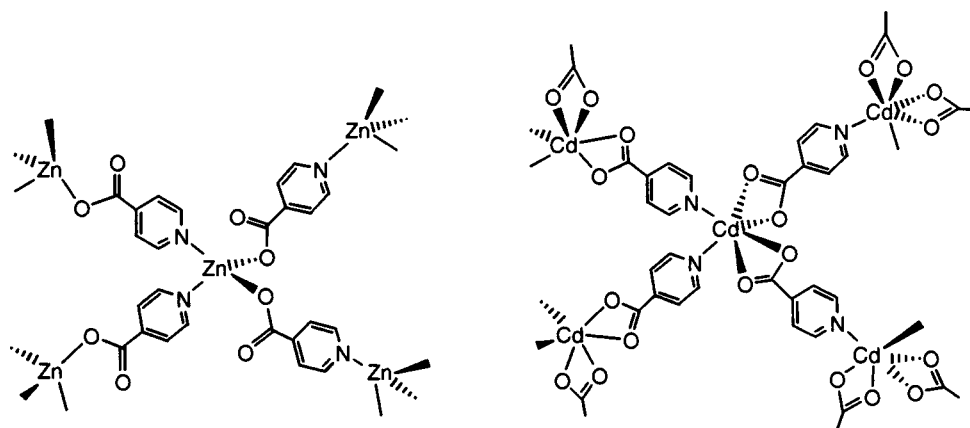
Wenbin Lin was born in Fujian, China. He received a B. S. degree from the University of Science and Technology of China, Hefei, Anhui in 1988 and came to the U.S. in 1989 to pursue his graduate studies under the guidance of G. S. Girolami and R. G. Nuzzo at the University of Illinois at Urbana–Champaign. Upon finishing his Ph.D. degree in 1994, he worked for T. J. Marks at Northwestern University on a NSF postdoctoral fellowship in the area of molecular self-assembly. Wenbin recently joined the faculty at University of North Carolina at Chapel Hill after four years as Assistant Professor at Brandeis University. His current research interests lie in the areas of crystal engineering, catalysis, chirotechnology, and materials chemistry.

A seemingly unorthodox approach to the crystal engineering of functional solids relies on the construction of polymeric networks. In this approach, a single strong interaction, such as hydrogen bonding or metal–ligand coordination, is utilized to assemble supramolecular networks with desired topologies from their constituent building blocks. Because a single strong interaction dominates in such systems, other weak intermolecular interactions play a less important role in the crystal packing. It is conceptually simpler to design appropriate molecular subunits (modules) to enhance the dominant hydrogen bonding or metal–ligand coordination interaction and, thus, induce the construction of noncentrosymmetric solids. The modular nature of such an approach also allows precise engineering of a multitude of properties via systematic tuning of the molecular modules. Since the properties of such solids are not only dependent upon the individual molecular components but are also a direct result of the arrangement of these constituents within the crystal lattice, these solids typically are not amenable to traditional characterization techniques developed for discrete molecules. Fortunately, single-crystal X-ray diffraction techniques have undergone revolutionary growth over the past few years and have helped develop supramolecular crystal engineering into an emerging field of interdisciplinary science. Notable examples include recent successful design of hydrogen-bonded lamellar frameworks based on guanidinium ion and various organosulfonates⁴ and construction of highly porous solids based on metal–organic coordination networks.⁵

Our interest in supramolecular crystal engineering has been primarily concerned with the rational design of noncentrosymmetric solids for applications in second-order nonlinear optics (NLO). Second-order NLO materials are key to the future photonics technology.⁶ There has been an intense research effort in second-order NLO materials over the past two decades, particularly in discrete organic molecular NLO chromophores.⁷ In such molecule-based NLO materials, the optical properties can be readily fine-tuned through subtle changes in the molecular structure using the tools of synthetic organic chemistry. Indeed, guided by theoretical models, many NLO chromophores with extremely high first hyperpolarizability (β) have been synthesized. However, to date, organic NLO materials have yet to find practical applications;⁷ inorganic materials such as lithium niobate and potassium dihydrogen phosphate (KDP) are exclusively used in electrooptic devices.⁶ The unsuitability of organic NLO materials for practical applications is primarily due to the requirement of noncentrosymmetric arrangements of molecular chromophores. Bulk second-order NLO susceptibility ($\chi^{(2)}$) is a third-rank tensor and will vanish in a centrosymmetric environment.⁸ Ideal NLO chromophores typically contain a good electron donor and acceptor connected through a conjugated bridge. Efficient NLO chromophores are, therefore, electronically asymmetric

* E-mail: wlin@unc.edu.

Scheme 1



and highly dipolar, and tend to adopt centrosymmetric arrangements as a result of the dominance of centrosymmetric dipole–dipole repulsions. To align NLO chromophores into a noncentrosymmetric bulk, several approaches, including poled-polymers,⁷ Langmuir–Blodgett films,⁹ and self-assembled multilayers¹⁰ have been explored. Despite tremendous progress in these areas, fabrication of organic NLO materials with high temporal and thermal stabilities remains a challenge.

Recent success in the design and synthesis of novel materials based on metal–organic coordination networks¹¹ has prompted us to examine supramolecular engineering of noncentrosymmetric solids by exploiting the strong and highly directional metal–ligand coordination bonds. We envision that coordination bonds can be utilized to counteract unfavorable centrosymmetric intermolecular interactions in the solid state. Noncentrosymmetric coordination networks with desired topologies can be rationally designed by taking advantage of well-defined metal coordination geometries in combination with carefully chosen rigid bridging ligands. We wish to describe in this Account our successful development of several crystal-engineering strategies toward the synthesis of noncentrosymmetric coordination networks and preliminary evaluation of their second-order NLO properties. We will divide this Account into three sections on the basis of the dimensionality of coordination networks: specifically, three-dimensional (3D) diamondoid networks,¹² two-dimensional (2D) grid structures,¹³ and one-dimensional (1D) and related helical systems.¹⁴

3D Diamondoid Networks. General principles governing the topologies of 3D coordination networks have recently been outlined by Robson et al.¹⁵ A coordination network is defined as a mathematical net or a series of metal connecting points (nodes) connected to a fixed number of bridging ligands (spacers). The crystal engineering of noncentrosymmetric coordination networks requires (a) identification of those nets that are not predisposed to pack in centrosymmetric space groups and (b) identification of potential nodes and spacers that can lead to the desired noncentrosymmetric topology.

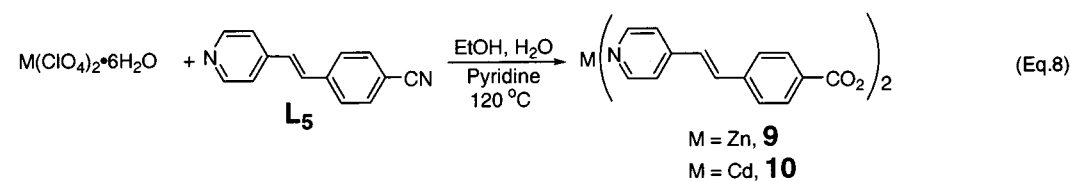
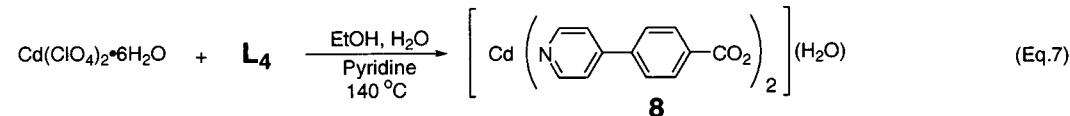
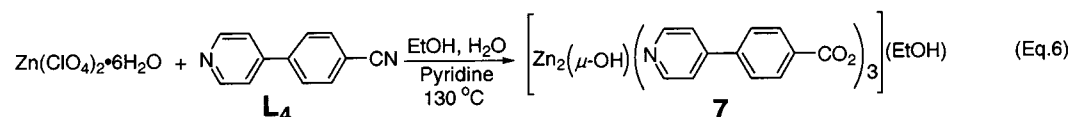
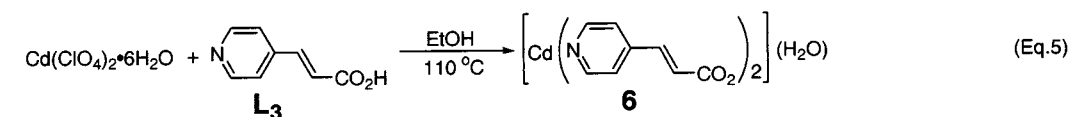
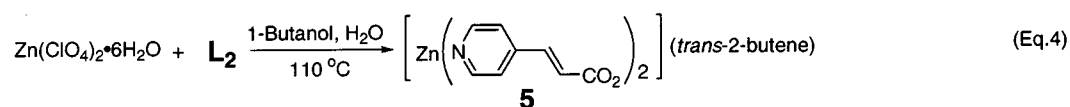
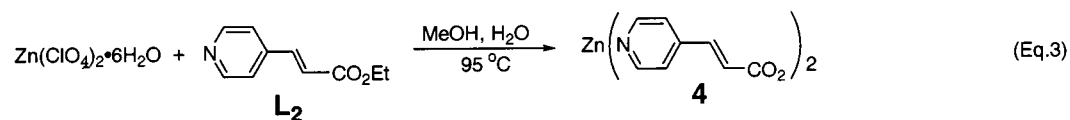
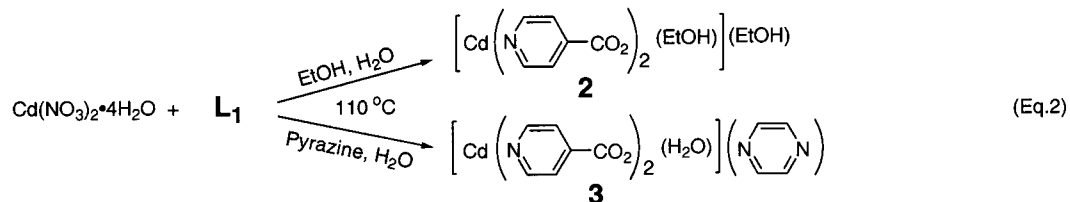
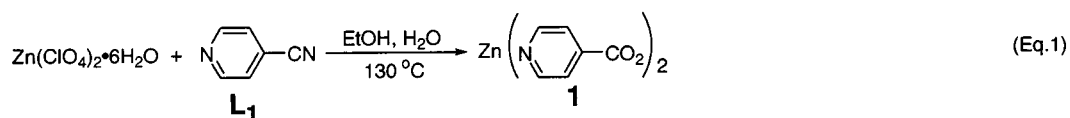
The most obvious choice of 3D network for crystal engineering of noncentrosymmetric solids is the diamon-

doid network (DN). Numerous metal–organic DNs have been synthesized over the past few years.¹⁶ DNs are not predisposed to pack in centrosymmetric space groups owing to the lack of inversion centers on the connecting points. In fact, the prototypical NLO material KDP crystallizes as a DN.¹⁷ We surmise that a noncentrosymmetric DN will arise if unsymmetrical bridging ligands are used to connect tetrahedral metal centers. It is also well-known that metal–organic DNs have a high propensity to interpenetrate in order to fill any void space.¹⁶ Despite the inherent noncentrosymmetric nature of individual DNs, an even-number-fold interpenetration could potentially lead to inversion centers relating pairs of mutually independent diamondoid nets. On the other hand, an *odd-number-fold interpenetrated DN synthesized from unsymmetrical bridging ligands will be necessarily noncentrosymmetric*.

Our preliminary work focused on the use of tetrahedral (or pseudotetrahedral) metal centers (nodes) and unsymmetrical rigid linear *p*-pyridinecarboxylate bridging ligands (spacers). The d^{10} metal ions Zn^{2+} and Cd^{2+} have been used as connecting points in order to avoid unwanted optical losses from $d \rightarrow d$ transitions in the visible region. When coordinated to both pyridyl and carboxylate groups (either in monodentate or chelating fashion) of the *p*-pyridinecarboxylate ligands, these d^{10} metal ions will have tetrahedral (or pseudotetrahedral) extension and, thus, have a high propensity of adopting DN structures (Scheme 1). Rigid conjugate bridging ligands have been chosen in order to minimize potential packing complexity due to ligand conformational flexibility. Furthermore, the use of an unsymmetrical linking group also introduces electronic asymmetry, and the rigidity of the bridging ligands is synergistic with good conjugation between the electron donors and acceptors. Both of these factors are necessary for second-order NLO effects.

We have taken advantage of hydro(solvo)thermal techniques to synthesize metal–organic DNs. Hydro(solvo)thermal synthesis provides an ideal condition for rapid growth of single crystals owing to lower solvent viscosity and facile diffusion processes under such conditions.¹⁸ Elevated temperatures during hydro(solvo)thermal syntheses also allow the formation of pyridinecarboxylate

Scheme 2



ligands from a wide variety of precursors (Scheme 2, **L**₁–**L**₅). We have demonstrated that the in situ slow hydrolysis of precursor ligands containing cyano or ester functionalities can result in less soluble phases not accessible from their corresponding acids by virtue of the presence of a large excess of metal ions under such synthetic conditions. X-ray diffraction-quality single crystals of metal–organic DNs have been readily obtained using hydro(solvo)-thermal techniques.

The first noncentrosymmetric DN bis(isonicotinato)-zinc, **1**, was synthesized from a hydro(solvo)thermal reaction between $\text{Zn}(\text{ClO}_4)_2 \cdot 6\text{H}_2\text{O}$ and 4-cyanopyridine (**L**₁) at 130 °C (eq 1).^{12a} An X-ray single-crystal structure determination reveals the formation of a 3-fold interpenetrated DN (Figure 1). Owing to the 3-fold interpenetration, **1** is necessarily noncentrosymmetric and, in fact, crystallizes in the chiral space group $P2_12_12_1$.

Subsequent reactions between $\text{Cd}(\text{NO}_3)_2 \cdot 4\text{H}_2\text{O}$ and **L**₁ in the presence of ethanol or pyrazine afforded $[\text{Cd}(\text{isonicotinato})_2(\text{EtOH})][\text{EtOH}]$, **2**, and $[\text{Cd}(\text{isonicotinato})_2(\text{H}_2\text{O})][\text{pyrazine}]$, **3**, respectively (eq 2).^{12b} In contrast to **1**, both **2** and **3** adopt a 2-fold interpenetrated DN, presumably owing to the tendency of Cd^{2+} ions to adopt a higher coordination number than Zn^{2+} ions (Figure 2). The coordination of a solvent molecule has prohibited the formation a 3-fold interpenetrated DN. The void space remaining after 2-fold interpenetration is effectively filled by included ethanol or pyrazine guest molecules. Both **2** and **3** contain a center of inversion relating the two independent networks and crystallize in the centrosymmetric space group $Pbca$. We have demonstrated that the framework structure of **2** could be maintained upon evacuation of ethanol guests to generate a microporous metal–organic solid.

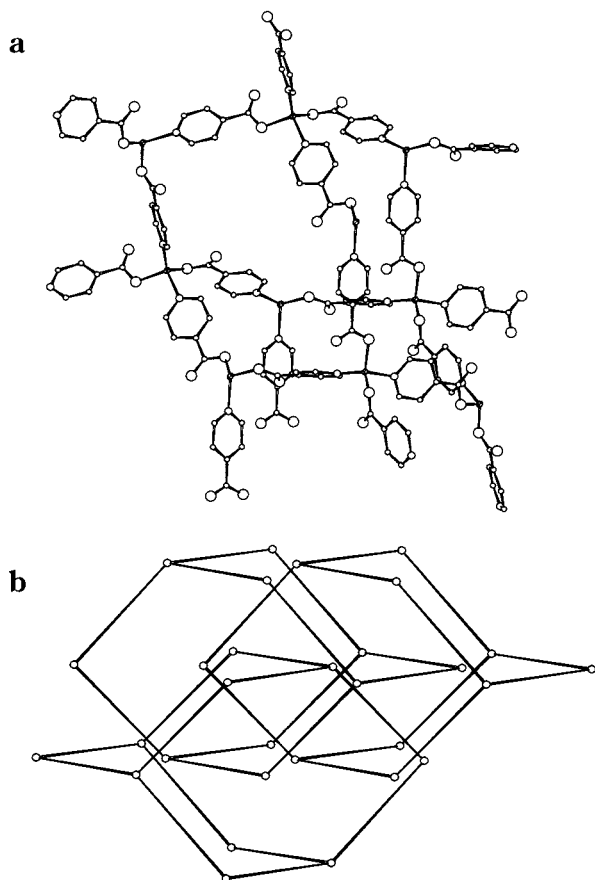


FIGURE 1. (a) Diamondoid network of **1**. (b) Diagram showing the 3-fold interpenetration in **1**.

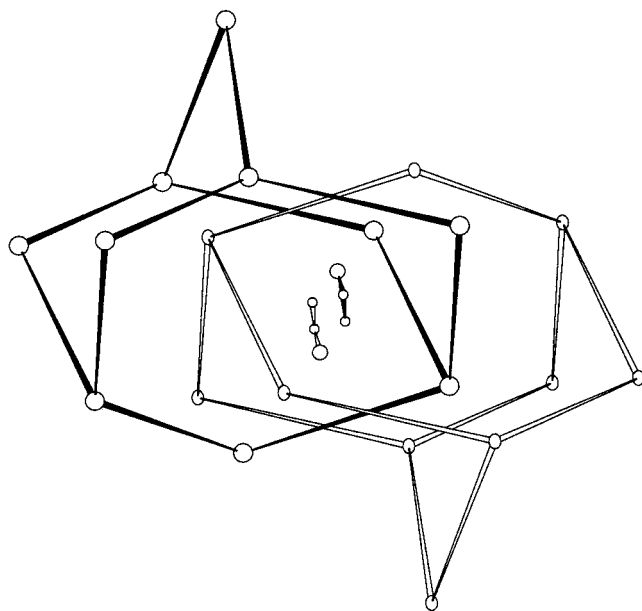


FIGURE 2. Diagram illustrating the 2-fold diamondoid network in **2**.

A hydro(solvo)thermal reaction of $\text{Zn}(\text{ClO}_4)_2 \cdot 6\text{H}_2\text{O}$ and L_2 in a mixture of methanol and water afforded $\text{Zn}(4\text{-pyridylacrylate})_2$, **4** (eq 3).^{12c} Compound **4** adopts a 5-fold interpenetrated DN and crystallizes in noncentrosymmetric space group Cc (Figure 3). Interestingly, when the reaction between $\text{Zn}(\text{ClO}_4)_2 \cdot 6\text{H}_2\text{O}$ and L_2 was carried out

in a mixture of 1-butanol and water, $[\text{Zn}(4\text{-pyridylacrylate})_2]\text{-}[trans\text{-}2\text{-butene}]$, **5**, was obtained (eq 4).^{12e} Compound **5** adopts a 4-fold diamondoid structure. The void space left after interpenetration is effectively filled by *trans*-2-butene guest molecules that formed from in situ dehydration of 1-butanol. As a result of 4-fold interpenetration, **5** crystallizes in the centrosymmetric space group $Pnna$.

A similar reaction between $\text{Cd}(\text{ClO}_4)_2 \cdot 6\text{H}_2\text{O}$ and L_3 in ethanol afforded $[\text{Cd}(4\text{-pyridylacrylate})_2](\text{H}_2\text{O})$, **6** (eq 5).^{12c} Compound **6** adopts a 5-fold interpenetrated DN with a similar topology as **4**. It is interesting to note that although the network topologies of compounds **2** and **3** seem to be sensitive to changes in the local metal coordination environments, the network topologies of **4** and **6** seem to be unaffected. These results may be attributed to the longer length of L_3 and, hence, slightly increased flexibility of the linking group. This flexibility allows slight distortions in the DN, thereby accommodating similar network topologies for both Zn^{2+} and Cd^{2+} ions.

In an effort to delineate the relationship between ligand length and degree of interpenetration, we have synthesized *p*-pyridinecarboxylate precursor L_4 via a Stille coupling reaction between 4-trimethylstannylpyridine and 4-bromobenzonitrile. A reaction of $\text{Zn}(\text{ClO}_4)_2 \cdot 6\text{H}_2\text{O}$ and L_4 in a mixture of water, pyridine, and ethanol afforded $[\text{Zn}_2(\mu\text{-OH})(4\text{-}(4\text{-pyridyl})\text{benzoate})_3][\text{EtOH}]$, **7** (eq 6).^{12c} The dizinc unit in **7** adopts a pseudotetrahedral arrangement of 4-(4-pyridyl)benzoate linking groups. Each dizinc unit is thus connected to four adjacent dizinc units to form a DN via two distinct linking groups. Two of the four linking groups are the expected unsymmetrical 4-(4-pyridylbenzoate) bridging ligands, and the other two are symmetrical bis[4-(4-pyridyl)benzoate] double bridges that are related by an inversion center. As a result, the individual DNs in **7** are inherently centrosymmetric. Compound **7** thus crystallizes in the centrosymmetric space group $P2_1/n$ despite 5-fold interpenetration. The formation of symmetrical bis[4-(4-pyridyl)benzoate] bridges in **7** is akin to using symmetrical 4,4-bipyridine or 1,4-benzenedicarboxylate as bridging groups. This result emphasizes the importance of unsymmetrical linking groups in the synthesis of noncentrosymmetric metal-organic frameworks

A similar reaction between $\text{Cd}(\text{ClO}_4)_2 \cdot 6\text{H}_2\text{O}$ and L_4 afforded $[\text{Cd}(4\text{-}(4\text{-pyridyl})\text{benzoate})_2](\text{H}_2\text{O})$, **8** (eq 7).^{12c} Compound **8** adopts the expected DN structure (Figure 4). Owing to the longer length of the 4-(4-pyridyl)benzoate groups versus the 4-pyridylacrylate groups, there is considerably more void space inside each DN of **8** than those of **4–6**. As a result, **8** adopts 7-fold interpenetration and crystallizes in the noncentrosymmetric space group Ia .

We have further extended this crystal engineering strategy to an even longer 4-[2-(4-pyridyl)ethenyl]benzoate bridging ligand.^{12d} Hydro(solvo)thermal reactions between $\text{M}(\text{ClO}_4)_2 \cdot 6\text{H}_2\text{O}$ and L_5 afforded $\text{M}\{4\text{-}[2\text{-}(4\text{-pyridyl})\text{ethenyl}]\text{benzoate}\}_2$ ($\text{M} = \text{Zn}$, **9**; $\text{M} = \text{Cd}$, **10**) (eq 8). The Zn centers in **9** adopt both tetrahedral and octahedral coordination environments, and the Cd centers in **10** adopt only octahedral environments. Despite the different metal coordination environments, both **9** and **10** adopt 8-fold

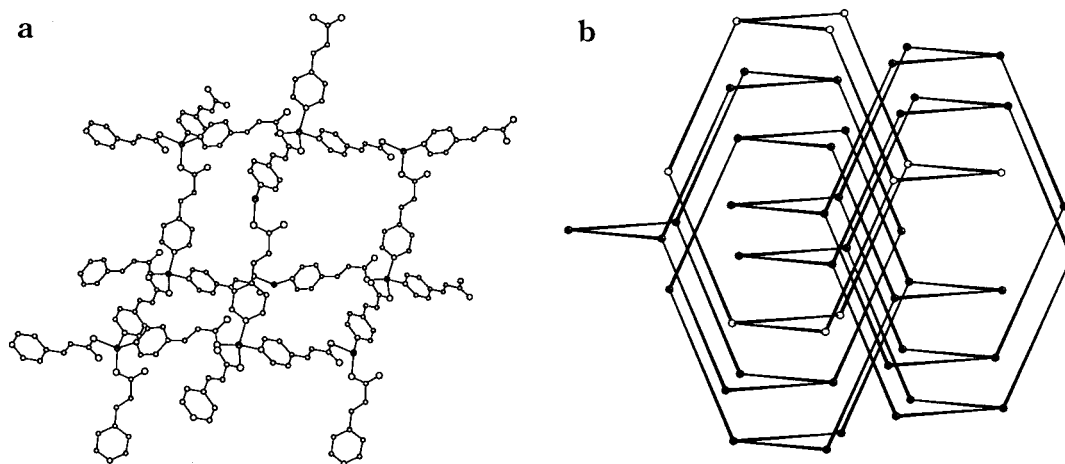


FIGURE 3. (a) Diamondoid structure of **4**. (b) Diagram illustrating the 5-fold interpenetration in **4**.

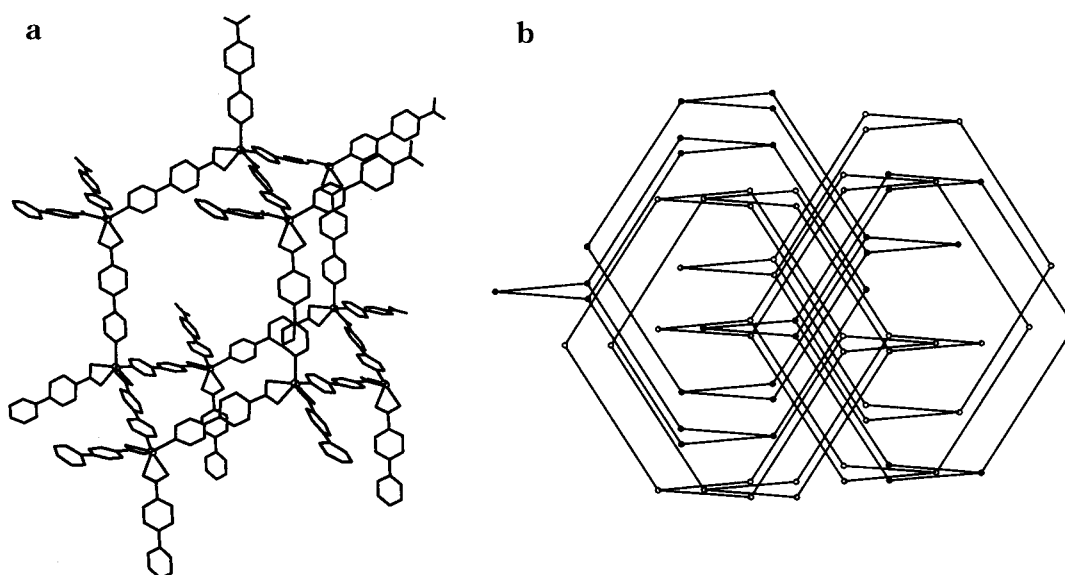


FIGURE 4. (a) One of the diamondoid networks in **8**. (b) Diagram illustrating the 7-fold interpenetration in **8**.

interpenetrated DNs with essentially the same network topologies (Figure 5). In fact, both **9** and **10** crystallize in the chiral space group $C2$ despite an 8-fold interpenetration. These results reinforce the notion that an even-number-fold interpenetration can, but may not, lead to the formation of centrosymmetric solids. Furthermore, the same network topology between **9** and **10** suggests that the formation of diamondoid solids depends mostly on the nature of the linking group, but is not sensitive to the local metal coordination environments. The similar network topology between **4** and **6** further supports this argument.

Our systematic study has convincingly demonstrated that metal *p*-pyridinecarboxylate frameworks have a high propensity to form diamondoid solids. Moreover, the combination of unsymmetrical bridging ligands and metal centers with appropriate geometry has led to the successful design of noncentrosymmetric solids. Although an even number-fold interpenetration can (but may not) introduce unwanted inversion centers and lead to bulk centrosymmetry, an odd-number-fold DN with unsymmetrical bridg-

ing ligands will necessarily crystallize in a noncentrosymmetric space group. Furthermore, there is compelling evidence to suggest that the degree of interpenetration is entirely dependent upon the length of the bridging ligand (Figure 6). Therefore, when armed with the versatility of organic synthesis, we can readily design ligands of the appropriate length to induce the formation of odd-number-fold interpenetrated DNs. We have, thus, for the first time conclusively demonstrated the crystal engineering of noncentrosymmetric solids based on 3D diamondoid coordination networks.

We have investigated the NLO properties of noncentrosymmetric diamondoid networks using the Kurtz powder techniques (Table 1).¹⁹ Measurements were carried out on ground samples with a particle size of $76 \pm 13 \mu\text{m}$ using a fundamental wavelength of 1064 nm. Consistent with their noncentrosymmetric structures, **1**, **4**, **6**, and **8–10** are SHG-active. In fact, the second-order NLO properties of **9** and **10** approach that of technologically important lithium niobate. These results are very encouraging, considering the limited donor/acceptor ability of *p*-

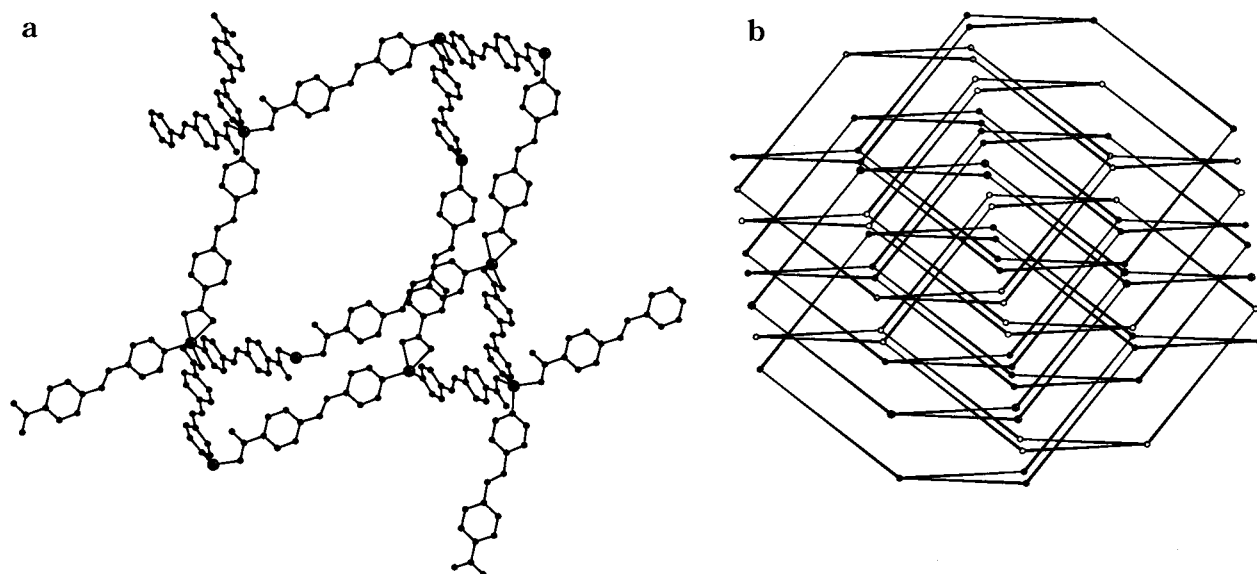


FIGURE 5. (a) Diamondoid network structure of **9**. (b) Diagram illustrating the interpenetration of eight independent diamondoid nets in **9**.

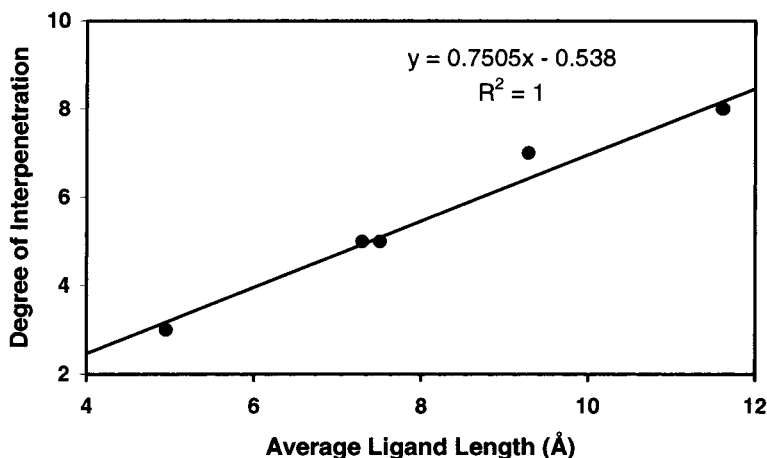


FIGURE 6. Dependence of degree of interpenetration of diamondoid networks on the length of bridging *p*-pyridinecarboxylate ligands.

Table 1. NLO Properties of Noncentrosymmetric Diamondoid Networks

compd	degree of interpenetration	space group	$I^{2\omega}/I^{\omega}$ (quartz)
1	3-fold	$P2_12_12_1$	1.5
4	5-fold	Cc	126
6	5-fold	Cc	18
8	7-fold	Ia	310
9	8-fold	$C2$	400
10	8-fold	$C2$	345
LiNbO ₃			600

pyridinecarboxylates. It is also obvious from Table 1 that increased ligand length results in enhanced SHG intensities. This correlation between SHG intensities and ligand lengths suggests that the electronic asymmetry in the *p*-pyridinecarboxylate ligands constitutes the molecular origin of second-order nonlinearities of these solids. Moreover, our work has demonstrated that efficient NLO materials can be synthesized with *modest* electron donor/acceptor combinations when all the constituents are efficiently aligned to function cooperatively. NLO materials based on metal–organic coordination networks are, therefore, advantageous in their transparency/nonlinearity

tradeoff. There is, thus, a great potential for further crystal engineering of noncentrosymmetric solids based on 3D diamondoid coordination networks for practical second-order NLO applications.

2D Coordination Networks. Our successful synthesis of noncentrosymmetric solids based on 3D DN has prompted us to explore other structural motifs. We hypothesize that the bent configuration of an *m*-pyridinecarboxylate ligand can accommodate the metal centers to adopt infinite 2D grid structures. The metal centers in either a *cis*-octahedral (with chelating carboxylate groups) or a tetrahedral (with monodentate carboxylate groups) environment can have at most C_{2v} symmetry and, thus, cannot possess an inversion center. When linked through unsymmetrical bifunctional bridging ligands, noncentrosymmetric 2D grids will result. The use of unsymmetrical *m*-pyridinecarboxylates also incorporates the electronic asymmetry necessary for second-order NLO properties. We have synthesized a series of noncentrosymmetric 2D grids from hydro(solvo)thermal reactions between *m*-pyridinecarboxylate precursors **L**₆–**L**₁₁ and transparent d¹⁰ metal centers.

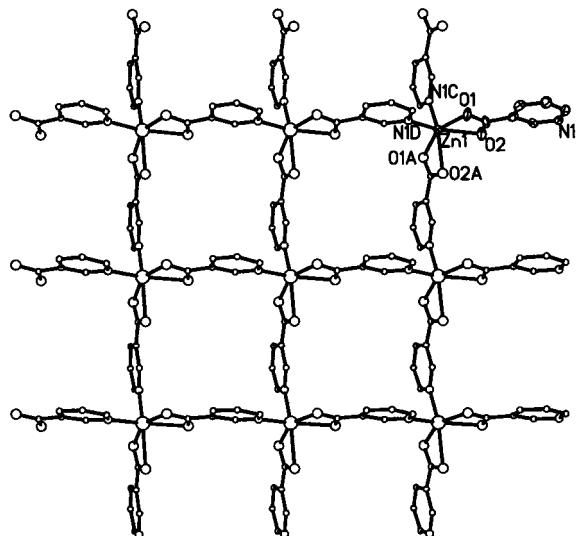


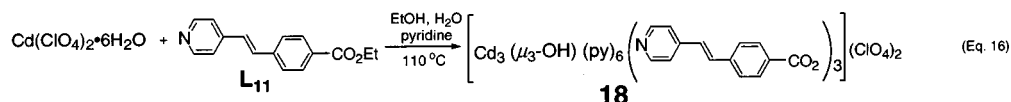
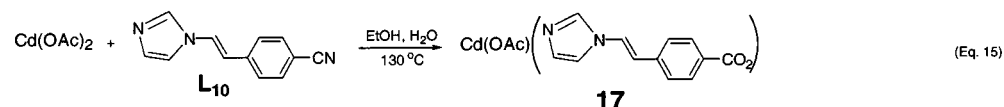
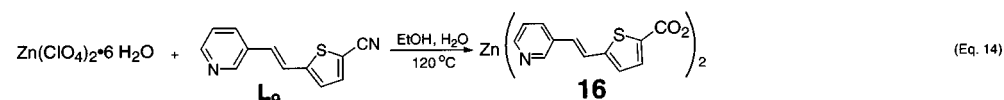
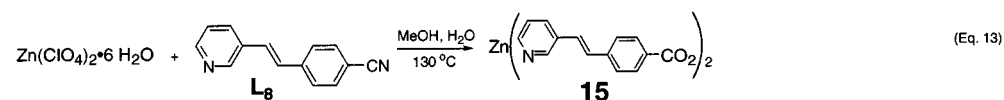
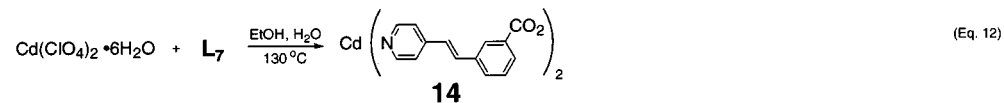
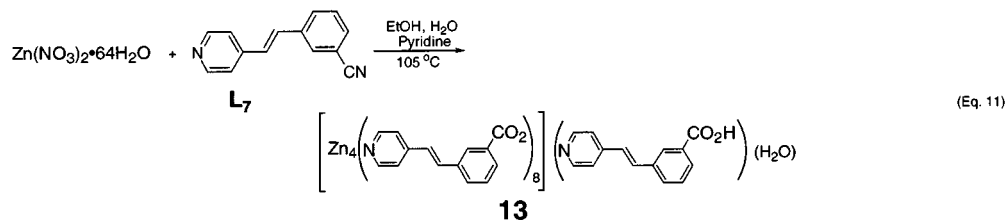
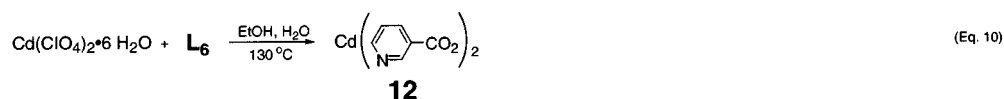
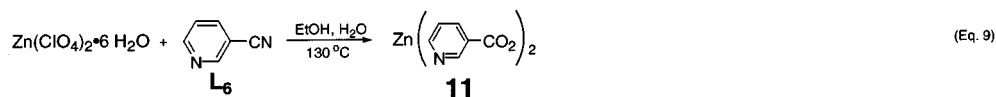
FIGURE 7. 2D square grid structure of **11**.

A hydro(solvo)thermal reaction between $\text{Zn}(\text{ClO}_4)_2 \cdot 6\text{H}_2\text{O}$ and L_6 afforded colorless crystals of $\text{Zn}(\text{nicotinate})_2$, **11** (eq 9).^{13a} The Zn centers in **11** adopt pseudo-octahedral geometry by coordinating to two carboxylate groups and

to two pyridyl nitrogen atoms of four different nicotinate groups in cis configuration. The Zn centers, thus, exhibit C_2 symmetry and are linked by nicotinate ligands to form a chiral infinite grid structure. Individual grids stack via interdigitation of 3-pyridyl groups to form a chiral solid that crystallizes in space group $P4_32_12$ (Figure 7). A similar reaction between $\text{Cd}(\text{ClO}_4)_2 \cdot 6\text{H}_2\text{O}$ and L_6 , however, resulted in a centrosymmetric solid bis(nicotinato)cadmium(II), **12**, which exhibits a complex 3D structure with bridging carboxylate groups (eq 10).^{13b} This result suggests that the formation of 2D grids can be affected by changes in the atomic radii of the metal connecting points.

A reaction of $\text{Zn}(\text{NO}_3)_2 \cdot 4\text{H}_2\text{O}$ and L_7 in a mixture of ethanol, water, and pyridine at 105°C affords colorless crystals of $\text{Zn}_4\{3\text{-}[2\text{-}(4\text{-pyridyl})\text{ethenyl}]\text{benzoate}\}_8 \cdot \{3\text{-}[2\text{-}(4\text{-pyridyl})\text{ethenyl}]\text{benzoic acid}\} \cdot (\text{H}_2\text{O})$, **13** (eq 11).^{13b} Compound **13** is built from four independent 2D grids that stack in an ABC-type sequence (Figure 8). Two of these rhombohedral grids exhibit 2-fold interweaving (A sequence) and the other two rhombohedral grids interdigitate through $\pi\text{-}\pi$ stacking (B and C sequences). The void space in **13** is, thus, filled through 2-fold interweaving and inclusion of a free 3-[2-(4-pyridyl)ethenyl]benzoic acid and

Scheme 3



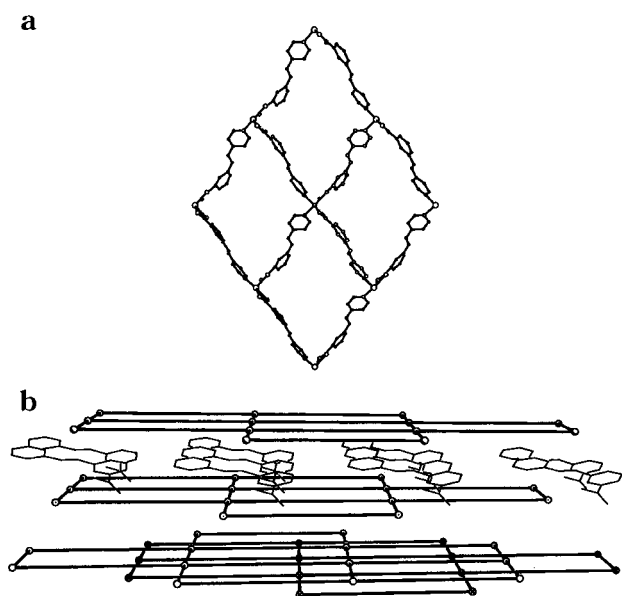


FIGURE 8. (a) 2D rhombohedral grid in **13**. (b) Stacking of four independent 2D rhombohedral grids along the *c* axis.

water guest molecules. The interweaving observed in **13** is common among 2D grids built from long bridging ligands and can potentially complicate the synthesis of noncentrosymmetric solids. An even-number-fold interweaving can also lead to unwanted inversion centers relating pairs of 2D grids. Despite the presence of 2-fold interweaving and inclusion of guest molecules, **13** fortunately crystallizes in the noncentrosymmetric space group *Cc*.

Interestingly, a similar reaction between $\text{Cd}(\text{ClO}_4)_2 \cdot 6\text{H}_2\text{O}$ and L_7 afforded $\text{Cd}\{3\text{-}[2\text{-}(4\text{-pyridyl})\text{ethenyl}]\text{benzoate}\}_2$, **14** (eq 12).^{13a} Compound **14** adopts the expected infinite 2D-grid structure and crystallizes in noncentrosymmetric space group *Fdd2* (Figure 9). Compound **14** exhibits 3-fold interweaving in order to fill the void space created by the longer ligand length within each 2D grid.

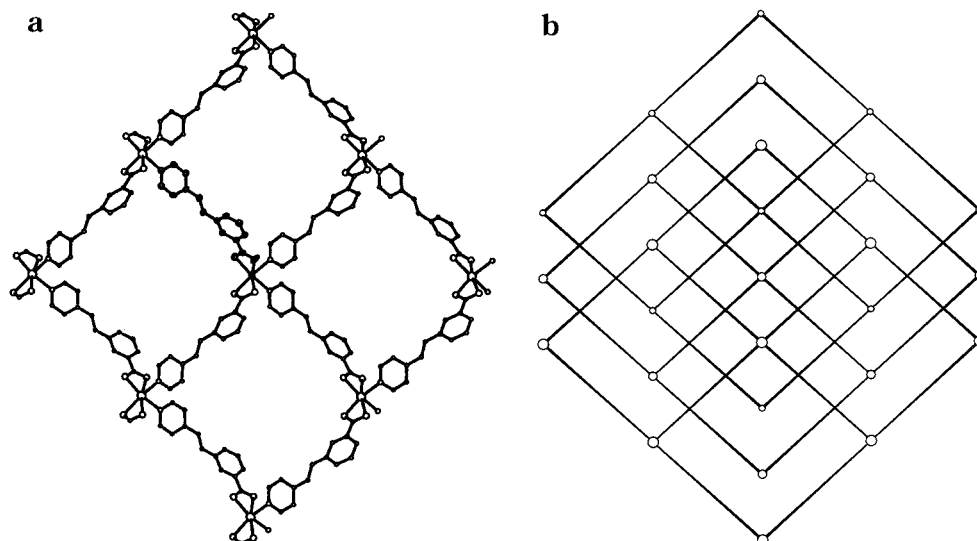


FIGURE 9. (a) 2D rhombohedral grid in **14**. (b) Schematic representation showing the interweaving of three independent rhombohedral grids in **14**.

A further examination of **14** also reveals that adjacent 3-fold interwoven grids are related via a glide plane. All the Cd centers within each 2D grid have the same *C2* chiral configuration. However, because of the presence of the glide plane, Cd centers in adjacent layers adopt opposite chirality to result in a supramolecular racemate. This result reveals an intrinsic problem in the development of crystal-engineering strategies based on 2D coordination networks. Specifically, although individual 2D networks can be designed to be necessarily noncentrosymmetric, stacking along the third dimension is still dictated by weaker noncovalent interactions. Such intermolecular interactions can force 2D coordination networks to adopt bulk centrosymmetry in which adjacent layers of 2D grids are related via inversion centers. It is, thus, necessary to develop novel packing arrangements that exhibit better interlayer registry and inhibit the occurrence of centrosymmetry. The pleated-sheet topology observed in **15–17** provides an interesting solution to such a problem.

$\text{Zn}\{4\text{-}[2\text{-}(3\text{-pyridyl})\text{ethenyl}]\text{benzoate}\}_2 \cdot (\text{H}_2\text{O})$, **15** was obtained by a reaction between $\text{Zn}(\text{ClO}_4)_2 \cdot 6\text{H}_2\text{O}$ and L_8 (eq 13).^{13b} Compound **15** adopts a highly distorted rhombohedral 2D grid structure with the Zn centers coordinating to two carboxylate groups in a monodentate fashion and to two pyridyl nitrogen atoms. Adjacent rows of Zn centers within each 2D grid are offset by 2.93 Å along the *c* axis to result in a pleated topology (Figure 10). The puckered nature of 2D grids renders better interlayer registry, and adjacent 2D grids are related only by translational symmetry. The Zn centers in **15**, thus, have the same chirality to lead to a chiral solid that crystallizes in space group *P2₁2₁2*. The pleated topology of **15** provides an effective means for controlling the stacking of 2D grids and represents an interesting structural motif for the synthesis of noncentrosymmetric 2D coordination networks. Similar pleated-sheet structures have been observed in $\text{Zn}\{5\text{-}[2\text{-}(3\text{-pyridyl})\text{ethenyl}]\text{thiophene-2-carbox-}$

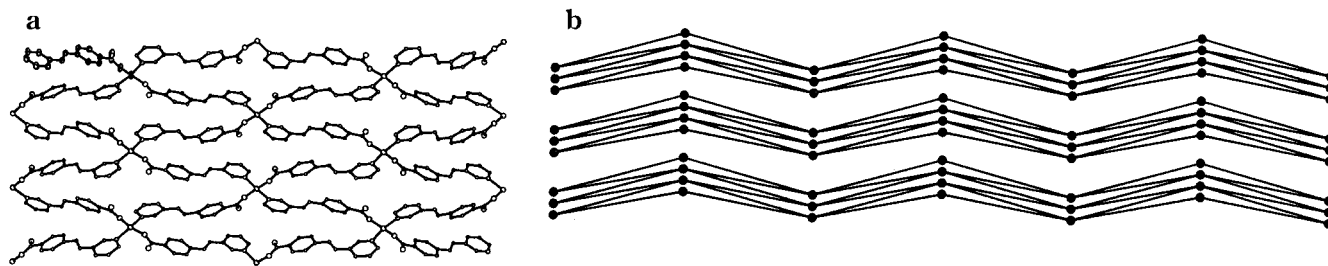


FIGURE 10. (a) 2D rhombohedral grid of **15**. (b) Stacking of adjacent 2D pleated sheets in **15**.

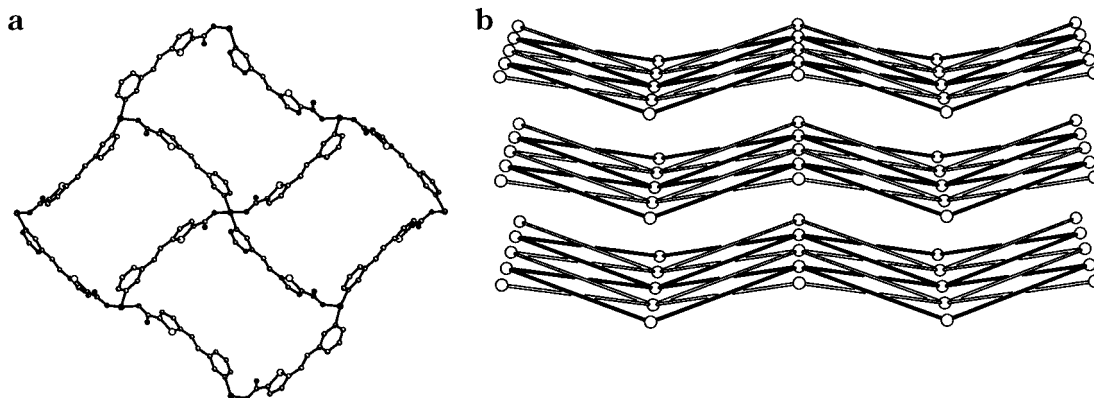


FIGURE 11. (a) 2D rhombohedral grid of **16**. (b) Schematic representation showing stacking of ruffled 2-fold interweaved 2D rhombohedral grids of **16**.

ylate)₂, **16**, and Cd(acetate){4-[2-(*N*-imidazolyl)ethenyl]-benzoate}, **17**.

Compound **16** was synthesized by a hydro(solvo)thermal reaction between Zn(ClO₄)₂·6H₂O and **L₉** (eq 14).^{13b} Similar to **15**, adjacent rows of Zn centers in each 2D grid of **16** are offset, resulting in a pleated topology (Figure 11). Compound **16**, however, adopts a 2-fold interweaved structure, and the two independent 2D grids are related by an inversion center. Compound **16** thus crystallizes in the centrosymmetric space group *Pcca*. Compound **17** was synthesized similarly from Cd(acetate)₂ and **L₁₀** (eq 15).^{13c} The presence of both bridging acetate and carboxylate groups has led to a centrosymmetric 2D grid structure that crystallizes in space group *Pcab*. The 2D grids in **17** are nonetheless highly puckered.

We have demonstrated the feasibility of crystal engineering noncentrosymmetric solids based on 2D grids; however, to ensure the noncentrosymmetry of bulk solid, not only the degree of interweaving, but also the stacking of 2D grids along the third dimension has to be carefully controlled. It is, therefore, significantly more challenging to engineer noncentrosymmetric solids based on 2D grids than on 3D DNs.

Powder SHG measurements indicated that compounds **11** and **13–15** are all SHG-active, in agreement with their noncentrosymmetric structures (Table 2). Compound **13** has a powder SHG intensity of 400 versus α -quartz, and **14** has a remarkable intensity of 800 versus α -quartz. For comparison, technologically important LiNbO₃ has a SHG intensity of 600 versus α -quartz. All of these 2D coordination networks are thermally robust and optically transparent, and they are, therefore, attractive candidates for practical NLO applications.

Table 2. Second-Order NLO Properties of Noncentrosymmetric 2D Networks

ocmpd	space group	$I^{2\omega}/I^{2\omega}$ (quartz)
11	<i>P</i> ₄ <i>3</i> <i>2</i> ₁ <i>2</i>	2
13	<i>Cc</i>	400
14	<i>Fdd</i> <i>2</i>	800
15	<i>P</i> ₂ <i>1</i> <i>2</i> ₁ <i>2</i>	sample decomp.
18	<i>R</i> <i>3</i> <i>2</i>	130
LiNbO ₃		600

We have recently successfully synthesized the first chiral octupolar metal–organic coordination network. It has been shown that donor/acceptor molecules with 3-fold rotational symmetry (octupolar chromophores) have four significant components of β and, thus, can have an improved transparency/optical nonlinearity tradeoff when compared to traditional dipolar chromophores.^{20,21} We have discovered that a hydro(solvo)thermal reaction between Cd(ClO₄)₂·6H₂O and **L₁₁** under basic conditions resulted in a novel octupolar 2D coordination network formulated as [Cd₃(μ -OH)(pyridine)₆(L_{11a})₃](ClO₄)₂, **18** (eq 16).^{13d} Compound **18** adopts an infinite 2D coordination network based on an unprecedented “basic” tricadmium carboxylate core (Figure 12). Unsymmetrical pyridine-carboxylate linking groups connect the tricadmium carboxylate clusters, resulting in a chiral infinite 2D layer. The 2D layers in **18** stack along the *c* axis in an interdigitated fashion, resulting in a chiral bulk solid (space group *R**3**2*). Kurtz powder SHG measurements indicated that **18** has a powder SHG intensity of 130 versus α -quartz, which is consistent with its chiral nature.

1D and Related Helical Coordination Networks. The design of noncentrosymmetric 1D chains can be readily achieved, but construction of a noncentrosymmetric solid

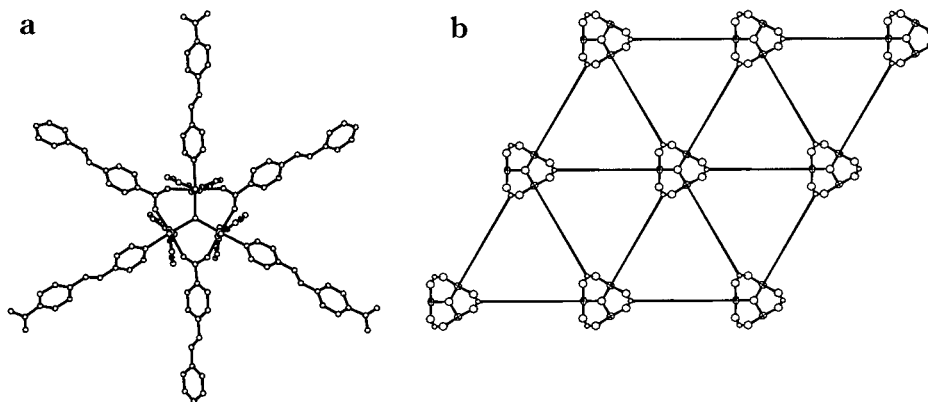
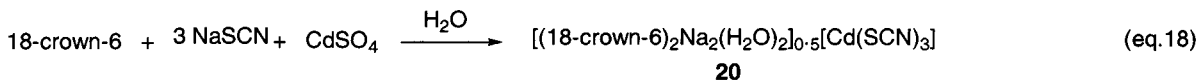
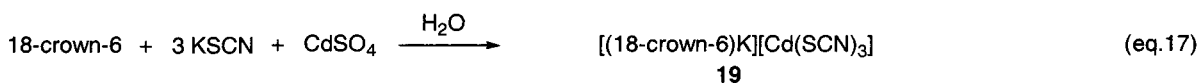


FIGURE 12. (a) View of the octupolar $[\text{Cd}_3(\mu_3\text{-OH})(\text{L}_{5a})_6(\text{py})_6]^{2+}$ building block in **18**. (b) Schematic representation showing the 2D $\{[\text{Cd}_3(\mu_3\text{-OH})(\text{L}_{5a})_3(\text{py})_6]^{2+}\}_n$ sheet in **18** down the c axis.

Scheme 4



R=Et, X=S (**21**), Se (**22**);
R=Me, X=S (**23**), Se (**24**)

based on 1D chains can be a formidable task owing to the lack of control in two other dimensions. Teo et al. recently developed an elegant approach to 1D NLO-active materials based on polymeric cadmium chalcogenocyanates.²² Anionic $[\text{Cd}(\text{XCN})_3]^-$ ($\text{X} = \text{S}$ or Se) chains are inherently noncentrosymmetric because strong trans effects force the chalcogen atoms to lie in positions trans to the nitrogen atoms (Scheme 4). The packing of the resulting individual $[\text{Cd}(\text{XCN})_3]^-$ chains, however, strongly depends on the symmetry of the cations. For instance, the cation in compound **20** is dimeric and contains an inversion center. As a result, **20** crystallizes in the centrosymmetric space group $P2_1/n$. On the other hand, the monomeric cation $[\text{18-crown-6}]\text{K}^+$ in **19** lacks an inversion center and leads to the formation of a noncentrosymmetric solid. The same cation dependence was observed in compounds **21–24**. The tetraalkylammonium cations in **21–24** do not possess inversion centers and lead to noncentrosymmetric solids. Compounds **19** and **21–22** have SHG efficiencies 1.5 to 3 times of KDP (KDP has a β^ω of ~ 10 versus α -quartz). However, **23** and **24** display negligible SHG efficiencies, because adjacent $[\text{Cd}(\text{XCN})_3]^-$ chains in **23** and **24** adopt an antiparallel arrangement to result in effective cancellation of dipole moments of individual chains which, in turn, nullifies any SHG effect.

We recently synthesized a novel noncentrosymmetric 1D coordination network with an interlocked structure $\text{Zn}-(4-[2-(4\text{-pyridyl})\text{vinyl}]\text{cinnamate})_2(\text{H}_2\text{O})$, **25**.^{14c} The asymmetric unit of **25** consists of one Zn center, one coordinated water, and two 4-[2-(4-pyridyl)vinyl]cinnamate groups. Although one of the ligands connects adjacent Zn

centers, resulting in 1D chains that run along the a axis, the other ligand only coordinates to the Zn center through a semichelating carboxylate group (with the pyridyl group noncoordinating). The dangling ligands form an intricate interlocking pattern via π - π stacking interactions that direct the packing of polar 1D chains into a noncentrosymmetric bulk solid (Figure 13).

Poepelmeier and co-workers have explored the synthesis of noncentrosymmetric solids based on transition metal oxyfluoride anions $[\text{MO}_2\text{F}_{6-x}]^{2-}$ ($\text{M} = \text{V}, \text{Nb}, \text{Ta}, x = 1$; $\text{M} = \text{Mo}, \text{W}, x = 2$).²³ Similar to the niobate anion in LiNbO_3 , $[\text{MO}_2\text{F}_{6-x}]^{2-}$ are inherently noncentrosymmetric because of a distortion of the metal from the center of the octahedron. Despite the noncentrosymmetric nature of $[\text{MO}_2\text{F}_{6-x}]^{2-}$ anions, they often crystallize in centrosymmetric space groups owing to orientational disorder of the oxyfluoride anions. Cocrystallization with two different cations has led to the ordering of the $[\text{MO}_2\text{F}_{6-x}]^{2-}$ anions. This technique effectively reduces the local symmetry about the $[\text{MO}_2\text{F}_{6-x}]^{2-}$ anion and the number of possible orientations, thereby promoting the formation of noncentrosymmetric 1D chains. But packing these anionic 1D chains into a noncentrosymmetric solid still remains a challenge. Poepelmeier and co-workers have recently met this challenge by synthesizing a helical metal-oxyfluoride $\text{Zn}(\text{pyrazine})(\text{H}_2\text{O})_2\text{MoO}_2\text{F}_4$, **26** (Figure 14). Widely found in nature, helical structural motifs exhibit axial chirality, and solids based on helical structural motifs can crystallize in noncentrosymmetric space groups. The $\text{MoO}_2\text{F}_4^{2-}$ anions in **26** are orientationally ordered and coordinated cis to $[\text{Zn}(\text{pyrazine})_2(\text{H}_2\text{O})_2]^{2+}$ cations in an

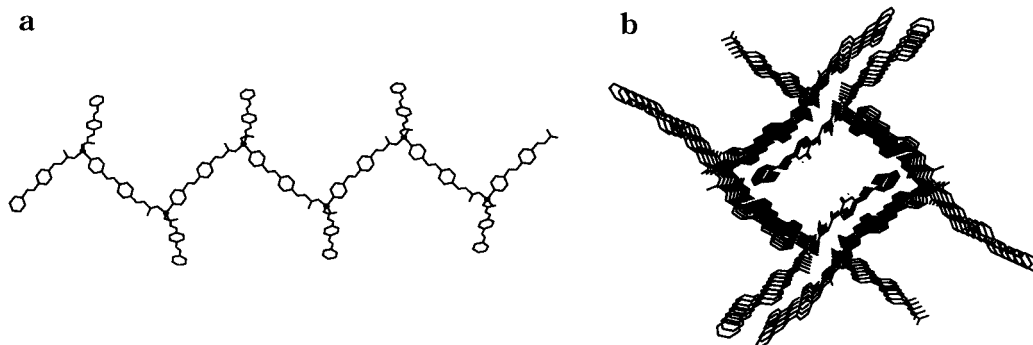


FIGURE 13. (a) 1D chain of **25**. (b) Perspective view showing the interdigitation of 1D chains in **25**.

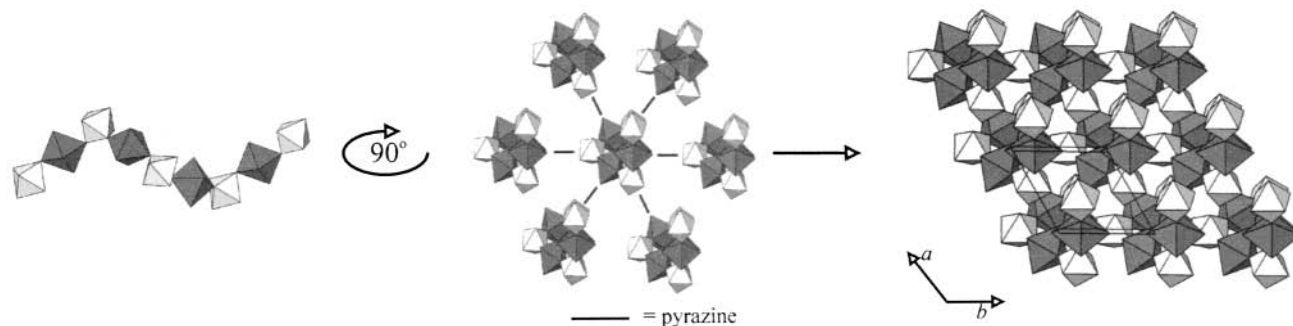


FIGURE 14. Polyhedral presentation of a helical chain of **26** and the linking of neighboring helices to form a chiral solid.

alternating fashion, resulting in 3_1 helical chains running along the c axis. All of the helices in **26** have the same handedness and are linked by pyrazine bridges, resulting in a 3D chiral solid.

We have also previously reported a chiral helical compound $\text{Zn}\{Z\text{-}[4\text{-}2\text{-}(3\text{-pyridyl})\text{ethenyl}]\text{benzoate}\}_2 \cdot 0.5\text{H}_2\text{O}$, **27**.^{14a} The skewed conformation of the bridging ligand in **27** has induced the formation of 6-fold helices. Just as in **26**, neighboring helices of **27** have the same handedness and are covalently bridged by pyridylethenylbenzoate ligands, resulting in a chiral 3D coordination network. Owing to nonconjugate nature of the Z conformation of the bridging ligand, **27** exhibits a modest powder SHG efficiency (I^{pow} of 6 vs α -quartz). The successful synthesis of **26** and **27**, thus, highlights the recurring theme of this Account: the probability of obtaining a noncentrosymmetric solid is significantly higher when it adopts a 3D framework structure.

Concluding Remarks. In this Account, we have outlined several successful strategies toward a new class of NLO materials based on polymeric metal–organic coordination networks. We have demonstrated the feasibility of crystal engineering of noncentrosymmetric solids by exploiting the strong and highly directional nature of metal–ligand coordination bonds. The key to our successful approaches lies in the utilization of dominant metal–ligand coordination to direct the assembly of supramolecular networks with desired topologies. The most successful strategy is based on 3D diamondoid networks. In such cases, we have effectively reduced the daunting task of crystal engineering of noncentrosymmetric solids to a simple choice of bridging ligands with appropriate length. The synthesis of noncentrosymmetric

coordination networks with lower dimensionality is less predictable. For example, centrosymmetry in 2D grids can arise from an even-number-fold interweaving as well as from the stacking of noncentrosymmetric sheets through centrosymmetric symmetry operations. We have shown that well-chosen metal centers and bridging ligands can lead to pleated sheets with an odd-number-fold interweaving, which will necessarily be noncentrosymmetric. Finally, noncentrosymmetric solids based on 1D and related helical networks can also be synthesized, albeit with much less predictability. Noncentrosymmetric coordination networks have a favorable combination of thermal and chemical stability, solubility characteristics, transparency, and second-order optical nonlinearity, and are, thus, potential candidates for applications in electrooptic devices. The present work serves as a nice example in which functional solid-state materials can be rationally designed.

We thank Dr. Zhiyong Wang, Ms. Ling Ma, Dr. Ponnaiyan Ayyappan, and Mr. Gergely Sirokman for their valuable contributions, Prof. Bruce M. Foxman for helpful discussions, and Prof. I. Y. Chan for help with SHG measurements. We also thank Dr. Scott R. Wilson and Ms. Teresa Prussak-Wieckowska for collecting X-ray diffraction data. We acknowledge funding support from the National Science Foundation (DMR-9875544), the Arnold and Mabel Beckman Foundation, the Alfred P. Sloan Foundation, Research Corporation, and the Camille and Henry Dreyfus Foundation.

References

- (1) (a) Desiraju, G. R. *Crystal Engineering: The Design of Organic Solids*; Elsevier: New York, 1999. (b) Lehn, J.-M. *Supramolecular Chemistry: Concepts and Perspectives*; VCH Publishers: New York, 1995.

- (2) Schmidt, G. M. J. Photodimerization in the solid-state. *Pure Appl. Chem.* **1971**, *27*, 647–678.
- (3) Gavezzotti, A. Are crystal structures predictable? *Acc. Chem. Res.* **1994**, *27*, 309–315.
- (4) Holman, K. T.; Pivovar, A. M.; Swift, J. A.; Ward, M. D. Metric engineering of soft molecular host frameworks. *Acc. Chem. Res.* **2001**, *34*, 107–118.
- (5) Eddaoudi, M.; Moler, D. B.; Li, H.; Chen, B.; Reineke, T. M.; O’Keeffe, M.; Yaghi, O. M. Modular chemistry: secondary building units as a basis for the design of highly porous and robust metal-organic carboxylate frameworks. *Acc. Chem. Res.* **2001**, *34*, 319–330.
- (6) (a) Bossi, D. E.; Ade, R. W. Integrated-optic modulators benefit high-speed fiber links. *Laser Focus World* **1992**, *28* (1), 135–142. (b) Higgins, T. V. Nonlinear crystals—where the colors of the rainbow begin. *Laser Focus World* **1992**, *28* (1), 125–133.
- (7) (a) Moerner, W. E.; Silence, S. M. Polymeric photorefractive materials. *Chem. Rev.* **1994**, *94*, 127–155. (b) Burland, D. M.; Miller, R. D.; Walsh, C. A. Second-order nonlinearity in poled-polymer systems. *Chem. Rev.* **1994**, *94*, 31–75. (c) Marks, T. J., Ratner, M. A. Design, synthesis, and properties of molecule-based assemblies with large second-order optical nonlinearities. *Angew. Chem., Int. Ed. Engl.* **1995**, *34*, 155–173.
- (8) Zyss, J. *Molecular Nonlinear Optics: Materials, Physics, and Devices*; Academic Press: New York, 1993. (b) Agulló-López, F.; Cabrera, J. M. Agulló-Rueda, F. *Electrooptics: Phenomena, Materials and Applications*; Academic Press: New York, 1994.
- (9) (a) Ashwell, G. J.; Jackson, P. D.; Crossland, W. A. Noncentrosymmetry and second-harmonic generation in Z-type Langmuir–Blodgett films. *Nature* **1994**, *368*, 438–440. (b) Penner, T. L.; Matschmann, H. R.; Armstrong, N. J.; Ezenyilimba, M. C.; Williams, D. J. Efficient phase-matched second-harmonic generation of blue light in an organic waveguide. *Nature* **1994**, *367*, 49–51.
- (10) (a) Lin, W.; Wong, G. K.; Marks, T. J. Supramolecular Approaches to Second-Order Nonlinear Optical Materials. Self-Assembly and Microstructural Characterization of Intrinsically Noncentrosymmetric [(Aminophenyl)azo]pyridinium Superlattices. *J. Am. Chem. Soc.* **1996**, *118*, 8034–8042. (b) Katz, H. E.; Wilson, W. L.; Scheller, G. Chromophore Structure, Second Harmonic Generation, and Orientational Order in Zirconium Phosphonate/Phosphate Self-Assembled Multilayers. *J. Am. Chem. Soc.* **1994**, *116*, 6636–6640.
- (11) (a) Zaworotko, M. J.; Moulton, B. From Molecules to Crystal Engineering: Supramolecular Isomerism and Polymorphism in Network Solids. *Chem. Rev.* **2001**, *101*, 1629–1658. (b) Hagman, P. J.; Hagman, D.; Zubieta, J. Organic–inorganic hybrid materials: from “simple” coordination polymers to organodiamine-templated molybdenum oxides. *Angew. Chem., Int. Ed.* **1999**, *38*, 2638–2684. (c) Munakata, M.; Wu, L. P.; Kuroda-Sowa, T. Toward the construction of functional solid-state supramolecular metal complexes containing copper(I) and silver(I). *Adv. Inorg. Chem.* **1999**, *46*, 173–304. (d) Galan-Mascaros, J. R.; Dunbar, K. R. A microporous framework from a magnetic molecular square: [Co(HAT)Cl₂]₄ (HAT = 1,4,5,8,9,11-hexaazatriphenylene). *Chem. Commun.* **2001**, 217–218. (e) Miller, J. S. Organometallic- and organic-based magnets: new chemistry and new materials for the new millennium. *Inorg. Chem.* **2000**, *39*, 4392–4408. (f) Seo, J. S.; Whang, D.; Lee, H.; Jun, S. I.; Oh, J.; Jeon, Y. J.; Kim, K. A homochiral metal-organic porous material for enantioselective separation and catalysis. *Nature* **2000**, *404*, 982–986.
- (12) (a) Evans, O. R.; Xiong, R.-G.; Wang, Z.; Wong, G. K.; Lin, W. Crystal engineering of noncentrosymmetric diamondoid metal-organic coordination networks. *Angew. Chem., Int. Ed. Engl.* **1999**, *38*, 536–538. (b) Evans, O. R.; Wang, Z.; Xiong, R.-G.; Foxman, B. M.; Lin, W. Nanoporous, interpenetrated metal–organic diamondoid networks. *Inorg. Chem.* **1999**, *38*, 2969–2973. (c) Evans, O. R.; Lin, W. Crystal engineering of nonlinear optical materials based on interpenetrated diamondoid coordination networks. *Chem. Mater.* **2001**, *13*, 2705–2712. (d) Lin, W.; Ma, L.; Evans, O. R. NLO-active Zn(II) and cadmium(II) coordination networks with 8-fold diamondoid structures. *Chem. Commun.* **2000**, 2263–2264. (e) Zhang, J.; Lin, W.; Chen, Z.-F.; Xiong, R.-G.; Abrahams, B. F.; Fun, H.-K. The first 4-fold interpenetrating diamondoid framework that traps gaseous molecules: Zn[*trans*-3-(4-pyridyl)acrylate]₂(*trans*-2-butene)_n. *Dalton Trans.* **2001**, 1806–1808.
- (13) (a) Lin, W.; Evans, O. R.; Xiong, R.-G.; Wang, Z. Supramolecular engineering of chiral and noncentrosymmetric 2d networks. Synthesis, structures, and second-order nonlinear optical properties of bis(nicotinato)zinc and bis{3-[2-(4-pyridyl)ethenyl]benzoato}-cadmium. *J. Am. Chem. Soc.* **1998**, *120*, 13272–13273. (b) Evans, O. R.; Lin, W. Rational design of nonlinear optical materials based on 2d coordination networks. *Chem. Mater.* **2001**, *13*, 3009–3017. (c) Evans, O. R.; Ayyappan, P.; Lin, W. manuscript in preparation. (d) Lin, W.; Wang, Z.; Ma, L. A novel octunoncentrosymmetric metal-organic NLO material based on a chiral 2d coordination network. *J. Am. Chem. Soc.* **1999**, *121*, 11249–11250.
- (14) (a) Evans, O. R.; Wang, Z.; Lin, W. An unprecedented 3D coordination network composed of two intersecting helices. *Chem. Commun.* **1999**, 1903–1904. (b) Evans, O. R.; Lin, W. Towards rational synthesis of noncentrosymmetric solids. Synthesis and X-ray structures of cadmium(II) meta-pyridinecarboxylate coordination polymers. *J. Chem. Soc., Dalton Trans.* **2000**, *21*, 3949–3954. (c) Evans, O. R.; Ayyappan, P.; Sirokman, G.; Lin, W. Manuscript in preparation.
- (15) Batten, S. R.; Robson, R. Interpenetrating nets: ordered, periodic entanglement. *Angew. Chem., Int. Ed. Engl.* **1998**, *37*, 1460–1494.
- (16) (a) Prosperio, D. M.; Hoffman, R.; Preuss, P. Possible Hard Materials Based on Interpenetrating Diamond-like Networks. *J. Am. Chem. Soc.* **1994**, *116*, 9634–9637. (b) Hirsch, K. A.; Wilson, S. R.; Moore, J. S. A packing model for interpenetrated diamondoid structures—an interpretation based on the constructive interference of supramolecular networks. *Chem. Eur. J.* **1997**, *3*, 765–771. (c) Zaworotko, M. J. Crystal engineering of diamondoid networks. *Chem. Soc. Rev.* **1994**, 283–288.
- (17) Endo, S.; Chino, T.; Tsuboi, S.; Koto, K. Pressure-induced transition of the hydrogen bond in the ferroelectric compounds potassium dihydrogen phosphate and potassium dideuterium phosphate. *Nature* **1989**, *340*, 452–455.
- (18) Rabenau, A. The role of hydrothermal synthesis in preparative chemistry. *Angew. Chem., Int. Ed. Engl.* **1985**, *24*, 1026–1040.
- (19) Kurtz, S. K.; Perry, T. T. A powder technique for the evaluation of nonlinear optical materials. *J. Appl. Phys.* **1968**, *39*, 3798–3813.
- (20) Zyss, J.; Ledoux, I. Nonlinear optics in multinoncentrosymmetric media: theory and experiments. *Chem. Rev.* **1994**, *94*, 77–105.
- (21) (a) Wortmann, R.; Glania, C.; Krämer, P.; Matschiner, R.; Wolff, J. J.; Kraft, S.; Treptow, B.; Barbu, E.; Langle, D.; Gölitz, G. Nondinoncentrosymmetric structures with 3-fold symmetry for nonlinear optics. *Chem. Eur. J.* **1997**, *3*, 1765–1773. (b) Thalladi, V. R.; Brasselet, S.; Weiss, H.-C.; Bläser, D.; Katz, A. K.; Carrell, H. L.; Boese, R.; Zyss, J.; Nangia, A.; Desiraju, G. R. Crystal engineering of some 2,4,6-triaryloxy-1,3,5-triazines: octunoncentrosymmetric nonlinear materials. *J. Am. Chem. Soc.* **1998**, *120*, 2563–2577.
- (22) Zhang, H.; Wang, X.; Zhang, K.; Teo, B. K. Molecular and crystal engineering of a new class of inorganic cadmium-thiocyanate polymers with host–guest complexes as organic spacers, controllers, and templates. *Coord. Chem. Rev.* **1999**, *183*, 157–195 and references therein.
- (23) Maggard, P. A.; Stern, C. L.; Poeppelmeier, K. R. Understanding the role of helical chains in the formation of noncentrosymmetric solids. *J. Am. Chem. Soc.* **2001**, *123*, 7742–7743 and references therein.

AR0001012